**Atmospheric
Chemistry
and Physics**

Mesosphere-to-stratosphere descent of odd nitrogen in February–March 2009 after sudden stratospheric warming

S.-M. Salmi[1,2], P. T. Verronen[1], L. Thölix[1], E. Kyrölä[1], L. Backman[1], A. Yu. Karpechko[1], and A. Seppälä[1,3]

[1]Finnish Meteorological Institute, Helsinki, Finland
[2]Department of Physics, University of Helsinki, Helsinki, Finland
[3]British Antarctic Survey (NERC), Cambridge, UK

Abstract. We use the 3-D FinROSE chemistry transport model (CTM) and Atmospheric Chemistry Experiment Fourier Transform Spectrometer (ACE-FTS) observations to study connections between atmospheric dynamics and middle atmospheric NO_x ($NO_x = NO + NO_2$) distribution. Two cases are considered in the northern polar regions: (1) descent of mesospheric NO_x in February–March 2009 after a major sudden stratospheric warming (SSW) and, for comparison, (2) early 2007 when no NO_x descent occurred. The model uses the European Centre for Medium-Range Weather Forecasts (ECMWF) operational data for winds and temperature, and we force NO_x at the model upper altitude boundary (80 km) with ACE-FTS observations. We then compare the model results with ACE-FTS observations at lower altitudes. For the periods studied, geomagnetic indices are low, which indicates absence of local NO_x production by particle precipitation. This gives us a good opportunity to study effects of atmospheric transport on polar NO_x. The model results show no NO_x descent in 2007, in agreement with ACE-FTS. In contrast, a large amount of NO_x descends in February–March 2009 from the upper to lower mesosphere at latitudes larger than 60° N, i.e. inside the polar vortex. Both observations and model results suggest NO_x increases of 150–200 ppb (i.e. by factor of 50) at 65 km due to the descent. However, the model underestimates the amount of NO_x around 55 km by 40–60 ppb. According to the model results, chemical loss of NO_x is insignificant during the descent period, i.e. polar NO_x is mainly controlled by dynamics. The descent is terminated and the polar NO_x amounts return to pre-descent levels in mid-March, when the polar vortex breaks. The break-up prevents the descending NO_x from reaching the upper stratosphere, where it could participate in catalytic ozone destruction. Both ACE-FTS observations and FinROSE show a decrease of ozone of 20–30 % at 30–50 km from mid-February to mid-March. In the model, these ozone changes are not related to the descent but are due to solar activation of halogen and NO_x chemistry.

1 Introduction

In the stratosphere odd nitrogen ($NO_x = NO + NO_2$) is produced mainly by oxidation of nitrous oxide (N_2O). Significant production occurs also in the lower thermosphere, around 110 km, through photoionization of N_2 by extreme ultraviolet (EUV) and soft X-ray radiation. In the polar regions, another important and highly varying source of NO_x is ionizing energetic particle precipitation directly affecting a wide range of altitudes from the thermosphere down to the stratosphere (Barth, 1992; Vitt et al., 2000). Because NO_x loss is driven by photodissociation, in the absence of solar radiation NO_x is chemically long-lived and therefore strongly affected by atmospheric dynamics.

In the recent years, observations have shown that during winter times NO_x can be effectively transported downwards inside the polar vortex (Funke et al., 2005, 2007; Hauchecorne et al., 2007; Seppälä et al., 2007; Randall et al., 2009), after NO_x is produced by particle precipitation in the mesosphere-lower thermosphere (MLT). Although the satellite observations of NO_x often cover altitudes up to middle mesosphere only, the connection to lower thermospheric NO_x production has been established using VLF (Very Low-Frequency) radio propagation data in the case of the 2004 descent event (Clilverd et al., 2006). Previously it had already been suggested that NO_x transport could provide a connection mechanism between particle precipitation in the MLT region and stratospheric ozone (Solomon et al., 1982; Siskind et al., 1997; Callis and Lambet, 1998). Several recent studies based on atmospheric modelling support the importance of wintertime NO_x enhancements to middle

atmospheric composition (Vogel et al., 2008; Baumgaertner et al., 2009; Reddmann et al., 2010). Callis et al. (2000) suggested that changes in NO_x concentrations due to particle precipitation and variations in transport could have a comparable effect on the amount of ozone in the upper stratosphere as changes in UV radiation at lower latitudes. At middle to high latitudes this coupling between NO_x and ozone may have a significant effect, again comparable in magnitude to that of UV radiation, also on the dynamics (Callis et al., 2001; Langematz et al., 2005). It has even been suggested that these changes could affect the polar regional ground-level climate although the linking mechanisms are not yet understood (Rozanov et al., 2005; Seppälä et al., 2009; Baumgaertner et al., 2010). Also other mechanisms connecting geomagnetic activity and middle atmospheric dynamics have been proposed. Arnold and Robinson (2001) suggested a coupling of geomagnetic activity to atmospheric waves. Lu et al. (2008) suggested that geomagnetic and far-UV perturbations might have an indirect connection to the stratosphere. Along the lines of Arnold and Robinson (2001), Lu et al. (2008) also concluded that this is likely due to coupling between the mean flow and atmospheric waves. Satellite observations have shown that exceptionally strong NO_x descent events occurred in 2004, 2006 and 2009 after sudden stratospheric warming events (Randall et al., 2009; Manney et al., 2009). These events are related to reformation of the vortex following its split/displacement. One of the strongest major SSWs on record occurred in the Northern Hemisphere in January 2009 (Manney et al., 2009). According to observations of the Microwave Limb Sounder (MLS), the stratopause broke down in late January and then reformed at very high altitudes around 80 km. During the major SSW the polar vortex split, but reformed after the SSW in the upper stratosphere where it became stronger than it initially was. Randall et al. (2009) used ACE-FTS data and showed that following the SSW stratospheric NO_x increased due to strong downward transport by factor of approximately 50 compared to winters without descent events. Because geomagnetic activity was low at the time, indicating that there was no significant NO_x production by particle precipitation occurring, the NO_x enhancement in 2009 was likely driven by the meteorology. Randall et al. (2009) further concluded that significant effects on ozone were neither expected nor observed since the descending NO_x enhancements never reached altitudes where NO_x is most effective at catalytic ozone destruction. However, they also pointed out the limitations of these conclusions, which were based on data not covering the whole polar night region.

In this paper we analyse the dynamics and meteorology of the winter of 2009 in the northern polar region using ECMWF operational analyses. Building on the observational analysis of Randall et al. (2009), we use the FinROSE chemistry transport model (CTM) to simulate this winter and the strong descent event of NO_x. This is done by constraining the model NO_x by enforcing a time-dependent upper boundary condition (UBC) based on ACE-FTS observations between 75 and 85 km altitude. Compared to earlier studies of other NO_x descent events utilizing ECMWF data (e.g. Vogel et al., 2008; Reddmann et al., 2010), in this study we use ECMWF operational analyses for dynamics up to 80 km, which gives us the opportunity to study the NO_x descent starting as high as from the upper mesosphere. The 3-dimensional CTM used in this study provides a complete coverage of the polar area, which thus enables also the study of any possible changes in ozone concentrations not seen by ACE-FTS due to its limited spatial coverage. For comparison, we also simulate the winter of 2007 when no comparable SSWs or NO_x descent was observed.

2 Model and measurements

2.1 Chemistry transport model FinROSE

FinROSE is a global 3-dimensional CTM designed for middle atmospheric studies (Damski et al., 2007). The model dynamics (i.e. temperature, horizontal winds and pressure) are from external sources i.e. changes in atmospheric composition do not affect the model dynamics. Vertical wind is calculated inside the model by using the continuity equation. In this study FinROSE is run with 41 vertical levels (0–80 km), a horizontal resolution of $10° \times 5°$ and is driven by operational analyses from ECMWF. The analyses are based on ECMWF simulations of a general circulation model (GCM) using four dimensional data assimilation (4D-VAR). The horizontal resolution and the number of vertical levels in FinROSE can be modified depending on the resolution of the meteorological data. The model calculates distributions of 40 species and families taking into account both chemistry and dynamics. However, only to the long-lived constituents are transported. The model includes about 120 homogeneous reactions and 30 photodissociation processes. Chemical kinetic data, reaction rate coefficients and absorption cross-sections are taken from look-up-tables based on the Jet Propulsion Laboratory compilation by Sander et al. (2006), including updates from the available supplements. Photodissociation frequencies are calculated using a radiative transfer model (Kylling et al., 1997). In addition to homogeneous chemistry, the model also includes heterogeneous chemistry, i.e. formation and sedimentation of PSCs and reactions on PSCs. Chemistry is not defined in the troposphere, but the tropospheric abundances are given as boundary conditions. At the lower boundary, monthly averages from ECMWF are used for ozone and water vapour, while methane is relaxed towards climatological distribution and other long-lived trace gases towards long time trends.

2.2 Observations

We have used observations from the FTS (Fourier Transform Spectrometer) instrument onboard the ACE satellite
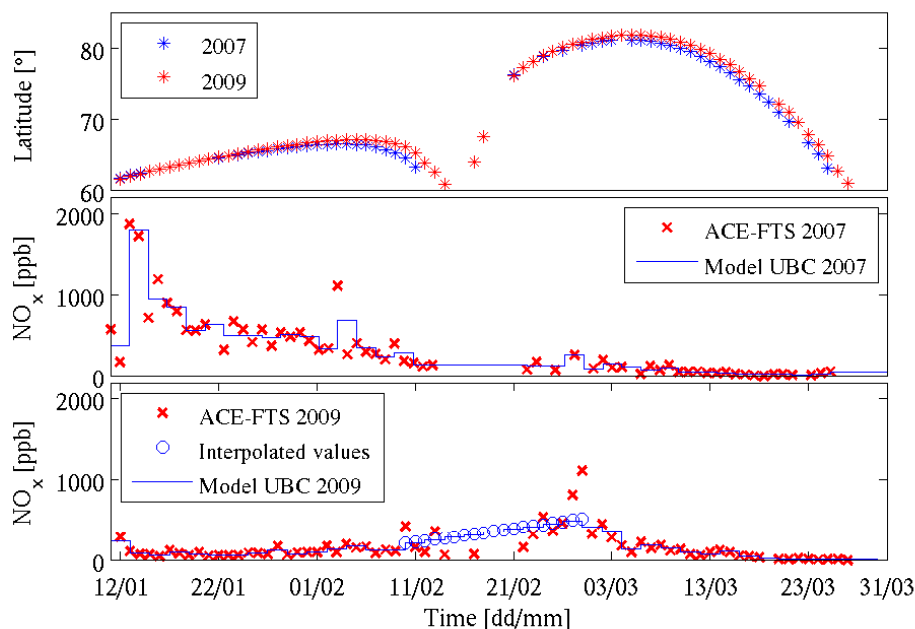
Fig. 1. Daily medians of ACE-FTS measurement locations north of 60° N (top) in 2007 (blue asterisk) and 2009 (red asterisk). The figure also shows mean NO$_x$ concentrations measured by ACE-FTS between 75–85 km altitudes (red crosses) and two-day means calculated from the observations (blue line) for 2007 (middle) and 2009 (bottom). Two-day means for 2009 are based on interpolated values between 10 and 28 February (blue circles).

(Atmospheric Chemistry Experiment) (Bernath et al., 2005). ACE-FTS is a solar occultation instrument launched in 2003. The instrument operates in the wavelength region of 2.2–13.3 µm and measures vertical profiles of temperature, pressure, density and 18 atmospheric constituents in the altitude range of 10–150 km. Figure 1 shows the daily medians of the measurement locations north of 60° N in January–March 2007 and 2009. We have calculated the median only when there are at least five measurements available during a day. Otherwise the measurements for that particular day have been neglected. In most cases ACE-FTS makes about 10 measurements per day. The figure also shows that the measurements represent almost the same latitudes from year to year. Measuring error for NO$_x$ depends on altitude and concentration (not shown) so that at 80 km altitude the error is 1–3 % for mixing ratios such as in late February–early March in 2009 and increases up to 10–15 % for NO$_x$ amounts observed in January 2009.

In this study we use ACE-FTS observations of NO$_x$ as an UBC for FinROSE (Fig. 1). We first calculated daily medians from the observations northward of 60° N for 2007 and 2009. As a result we got one value per day representing approximately a zonal average at the median latitude. Using these daily values we then calculated two-day means, which we in this study use at the upper boundary of the model. This two-day mean value is used on every time step for two days after which the next two-day mean is used. In case of missing data for both of the days in question, we use the

previous two-day mean. The UBC is taken uniform at every grid point between 60° N–90° N. It should be noted that the instrument changed the direction of the measurements towards lower latitudes after the 5 February, which can be seen as a decrease of about 400 ppb in the 2009 NO$_x$ mixing ratios (Fig. 1). Around 16 February ACE-FTS continued measuring on northern latitudes (>60° N) and NO$_x$ concentrations increased because of this. The effect can be seen as a minimum in the 2009 NO$_x$ mixing ratios between 10 and 28 February in Fig. 1. This means that the ACE-FTS measurements do not give a representative general view of the situation in the polar region during this time period. To reduce the influence of the change in the measuring direction, we replaced the 2009 ACE-FTS observations with interpolated values over the minimum (blue circles in Fig. 1) and neglected the largest values. This is somewhat arbitrary, but perhaps the best approach taking into account the lack of usable data in this time period.

3 Results

3.1 Meteorological conditions

In this section we use the ECMWF operational data to analyse the meteorological conditions and their differences in early 2007 and 2009. We are aware of the possible shortcomings of the data (Manney et al., 2008), but for this study it is important that the ECMWF fields extend up to 80 km,
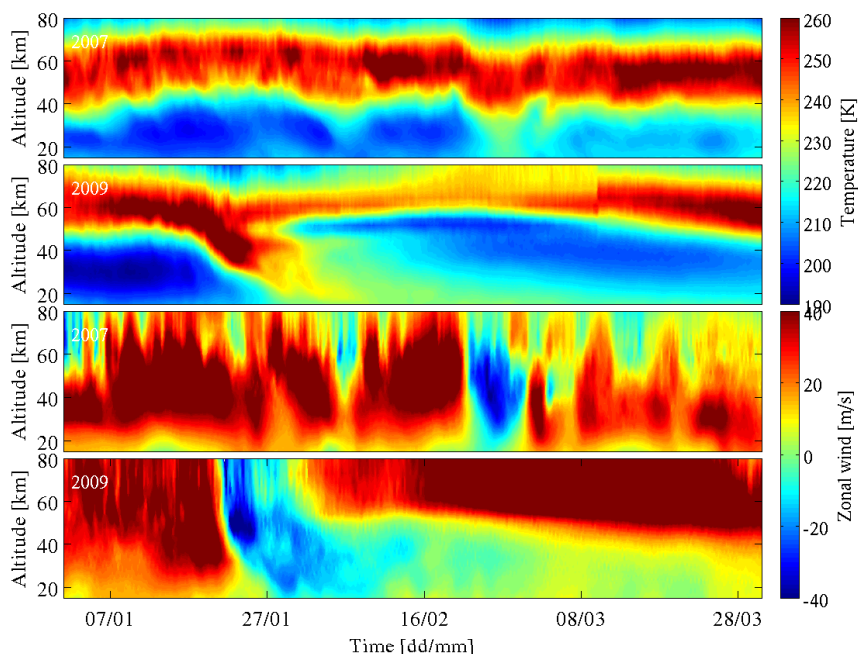
Fig. 2. ECMWF zonal mean temperature (K) and zonal mean zonal wind (m s^{-1}) at 75° N as a function of time and altitude for winters 2007 and 2009.

allowing us to model the NO$_x$ descent starting as high as from the upper mesosphere.

Figure 2 shows zonal mean temperature (two top panels) and zonal mean zonal wind (two bottom panels) at 75° N for 2007 and 2009 as a function of time and altitude. The meteorological conditions show remarkable differences between these two years. The winter of 2007 was rather stable whereas early 2009 was dynamically quite exceptional as the stratopause warmed and dropped below 30 km in late January. In early February the stratopause reformed around 80 km, which led to very low temperatures between 30 and 50 km. The same figure also shows that the warming in 2009 was accompanied by a rapid change in the direction of the zonal flow (from positive/westerly to negative/easterly), which persisted until early March. This one month period of easterly winds in 2009 led to low wave activity above the critical level, which for stationary waves corresponds to a level where the zonal wind speed equals to zero, and enabled the formation of a strong polar vortex, which did not break until early March. Changes in the wind direction took place also in early and late February 2007, but these changes lasted only for at most ≈10 days. Extreme changes in stratopause temperatures, as in 2009, did not occur.

According to McInturff (1978), the criteria for a major SSW are fulfilled when the latitudinal mean temperature at 10 hPa (≈30 km) or below increases poleward of 60° N and the zonal winds are reversed from westerly to easterly in the same area. Figure 3 shows the zonal mean temperature and zonal mean zonal wind at 10 hPa as a function of time and

latitude. The poleward temperature gradient reversed during both winters. In 2007 the temperature increase was fairly small (≈10 K) and lasted only about 10 days. The warming in 2009 was more pronounced and the temperature gradient was positive for approximately 20 consecutive days in the polar region. The figure also shows that the zonal mean wind at 10 hPa reversed from westerly to easterly at the same time when the temperature gradient became positive. This indicates that a major SSW occurred in both winters. However, the situation in 2007 returned to undisturbed winter conditions in a few days, which is more common for minor SSWs. In 2009 the wind reversal to westerly took about one month, giving enough time for the vortex to recover in the upper stratosphere/lower mesosphere. The criteria for a major SSW in 2009 were first met on the 24 January (black vertical dashed line).

It has been suggested by Manney et al. (2008) that the ECMWF operational analyses underestimate the variations in the stratopause altitude during extreme meteorological conditions. The operational analyses agree, however, well with satellite observations of MLS and SABER (Sounding of the Atmosphere using Broadband Emission Radiometry) in early winter stratopause temperatures. Compared to the MLS measurements (Manney et al., 2009) the ECMWF operational analyses underestimate the altitude of the stratopause reformation in 2009 by about 5 km. The zonal wind, instead, resembles MLS measurements also at higher altitudes. Below 50 km altitude the MLS observations and operational analyses are in very good agreement.
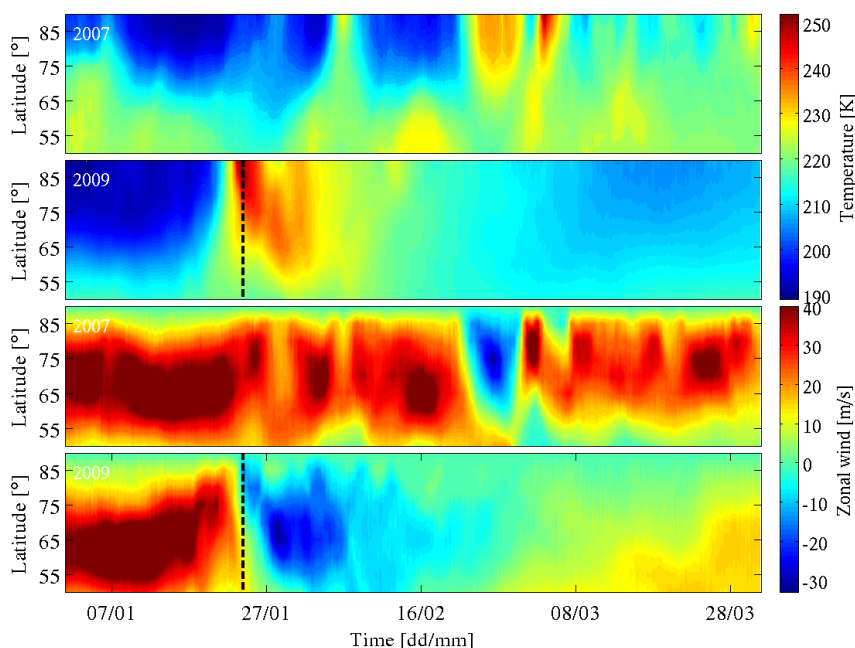
Fig. 3. ECMWF zonal mean temperature (K) and zonal mean zonal wind (m s^{-1}) at 10 hPa ($\approx$30 km) as a function of time and latitude. The vertical black dashed lines in figures representing the year 2009 show the date when the criteria for the major SSW were fulfilled.

3.2 NO$_x$ descent

Figure 4 presents NO$_x$ observations measured by ACE-FTS in 2007 (top) and 2009 (bottom). Plotted are daily medians north of 60° N, which correspond to measurement locations shown in Fig. 1. The observations show that there were large differences in the distribution of NO$_x$ between years 2007 and 2009. In 2007 the mesospheric maximum of NO$_x$ reached 60–65 km in the beginning of the year and then ascended towards the spring. This can be explained by changes in the zonal mean temperature and wind fields (Figs. 2 and 3). The stratopause was quite stable until the beginning of February, when the temperatures increased for a few days and the westerly winds weakened. Warm midlatitude air with low NO$_x$ concentrations mixed with the colder polar air and decreased the NO$_x$ concentrations. This warming did not dislocate the stratopause and the temperatures remained quite high even after the warming. The warming in late February produced no significant effects on NO$_x$.

In contrast, the major SSW in 2009 had a great impact on NO$_x$. A tongue-like structure of descending NO$_x$ from the mesosphere to the stratosphere after the SSW is clearly seen in Fig. 4. High NO$_x$ amounts were transported from 80 to 55 km altitude in about 40 days. The descent took place during the recovery of the polar vortex and is also discussed by Randall et al. (2009). Comparison of NO$_x$ and isentrops calculated from ECMWF operational data indicates that the NO$_x$ concentration isolines crossed the isentrops (not shown), suggesting that the descent was diabatic. The situa-

tion is thus similar to the upper stratospheric vortex recovery that occurred after a SSW in winter 2005/2006 (Manney et al., 2008). In mid-March the descent stopped and NO$_x$ concentrations decreased back to the level on which they were before the SSW. At this time the stratopause had already reformed and the zonal winds had started to reverse back to westerly (Fig. 2) allowing planetary waves to propagate upward, interact with the vortex, and mix the low-NO$_x$ air from outside the vortex with high-NO$_x$ air inside the vortex.

Figure 5 shows NO$_x$ timeseries calculated from FinROSE-CTM results. The data are daily means, calculated using only the grid points corresponding to ACE-FTS measurement locations (Fig. 1). The model reproduces the distribution of NO$_x$ reasonably well compared to the observations shown in Fig. 4. The maximum of NO$_x$ in the beginning of 2007 at about 75 km is of the same order of magnitude (800–900 ppb) as in the observations, but extends 3–5 km lower in the middle atmosphere. In 2009, the observations and model results show an increase of NO$_x$ to 150–200 ppb at 65 km. The modelled and observed NO$_x$ both descend to about 55 km, but at this altitude the amount of NO$_x$ is underestimated in the model by 40–60 ppb. The descent also starts 3–5 days earlier and lasts 3–5 days longer in the model than in the observations.

In order to test the robustness of the results, we averaged the model NO$_x$ over the whole polar cap (60° N–90° N) instead of sampling at ACE locations, but found this to have only a slight effect on the results (not shown). Compared to the sampled results (Fig. 5) the descent stopped a couple
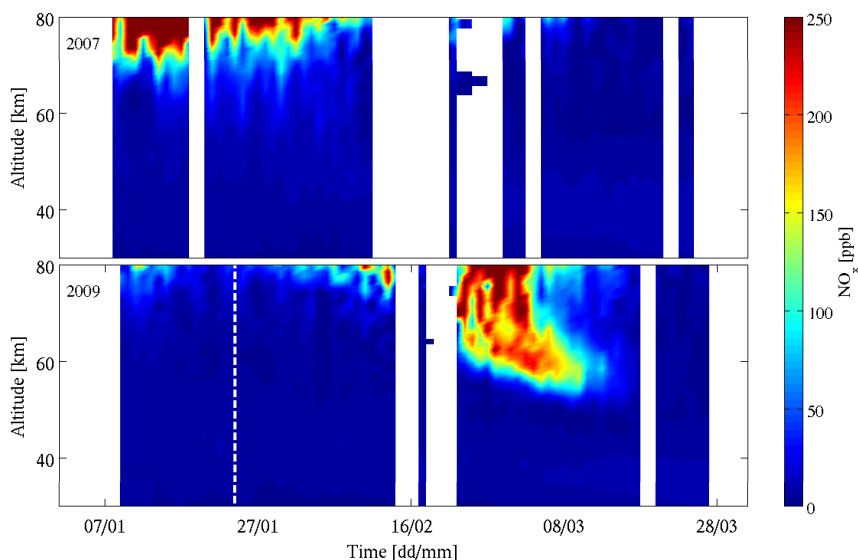
Fig. 4. NO$_x$ time series (ppb) as daily medians measured by ACE-FTS. White dashed line indicates the time point, when the criteria for the major SSW were fulfilled in 2009. The upper panel is for 2007 and the lower for 2009. White regions indicate missing data or not enough data.
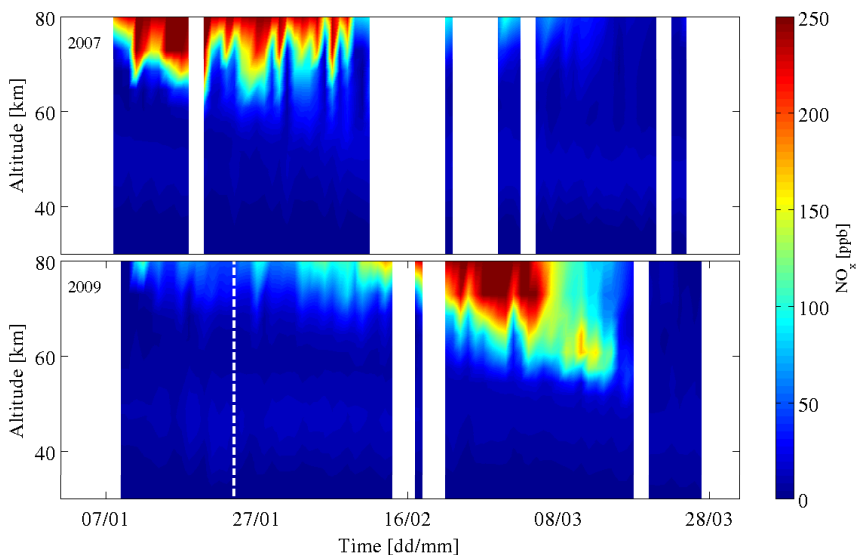

Fig. 5. NO$_x$ time series (ppb) as daily means from FinROSE-CTM. White dashed line indicates the time point, when the criteria for the major SSW were fulfilled in 2009. The upper panel is for 2007 and the lower for 2009. White regions indicate missing ACE-FTS data or not enough ACE-FTS data.

of days earlier above 60 km, but continued longer until late March between 60 and 50 km with NO$_x$ mixing ratios of 50–100 ppb. Otherwise the concentrations were of the same magnitude as in the sampled results. The similarity between the sampled and whole-polar-cap results from the model suggests that NO$_x$ did not reach upper stratosphere anywhere in the polar cap region.

To estimate the effect of different UBCs on the NO$_x$ descent we made two additional model runs. In these runs

we used the following upper boundaries: (1) a constant value ($\sim$670 ppb) between the 11 February and the 4 March and (2) a two-step increment of NO$_x$ so that the first step ($\sim$190 ppb) is located between the 11 and 21 February and the second one ($\sim$540 ppb) between the 22 February and the 4 March. The results (not shown) for case 2 are in agreement with those obtained with the interpolated upper boundary shown in Fig. 1. In contrast, case 1 produces about 100 ppb higher NO$_x$ mixing ratios between 60 and 80 km during the
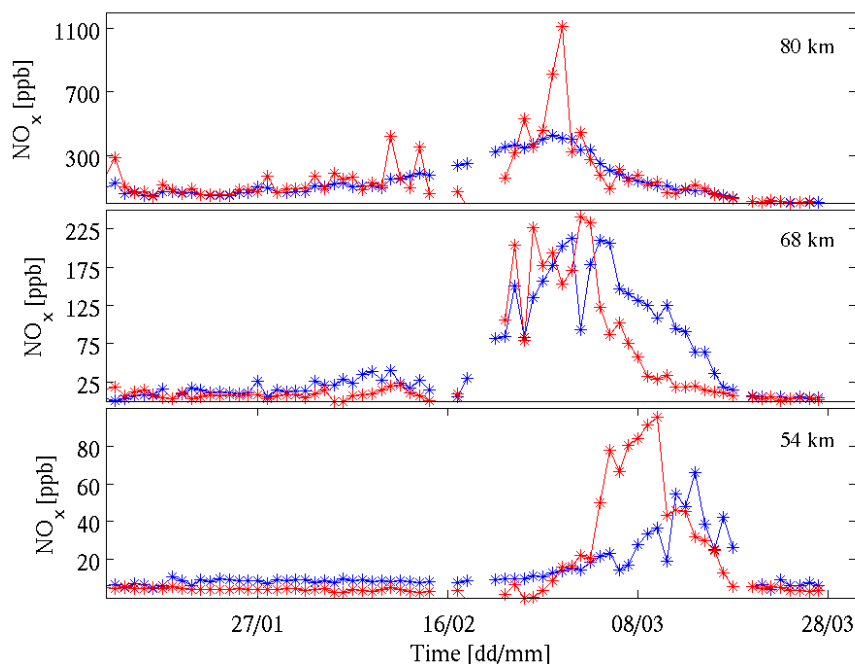
Fig. 6. ACE-FTS NO_x observations (red line) and model results (blue line) in ppb at 80 (top), 68 (middle) and 54 km (bottom) altitudes as a function of time in 2009.

descent event until early March. At this time the mixing ratios are about 50 ppb higher. However, NO_x descent stops at the same altitude as with the interpolated upper boundary. As expected, the different upper boundaries change only the amount of descending NO_x because in all model runs the descent is driven by the same ECMWF meteorological data.

Figure 6 shows the model results and ACE-FTS observations at 80, 68 and 54 km altitudes. Differences at 80 km altitude during 10–28 February are due to the interpolated UBC at that time. However, the modified UBC improves the agreement between the model and observations at lower altitudes. There is a reasonable agreement between the model and the observations at 68 km altitude. An overestimation of about 100 ppb occurs after the 8 March, consistent with the fact that the descent lasted longer in the model than observed by ACE-FTS. Significant differences are found at 54 km where the model produces 40–60 ppb smaller values than found in the observations. The observed maximum of NO_x occurs about 10 days earlier compared to the model results. Overall, the model succeds to reproduce the descent of NO_x, with no in-situ production included in the model, reasonably well compared to the observations and confirms the results of Randall et al. (2009) about the importance of dynamics on the distribution of NO_x. Although this is not a direct measure, the NO_x comparison suggest that the ECMWF data are in this case usable in atmospheric modelling also at mesospheric altitudes.

Figure 7 illustrates the modelled distribution of NO_x in the northern polar region (50° N–90° N). The descending NO_x reaches 69 km altitude already on 6 February with amounts of 80–100 ppb. The circular structure of NO_x in the polar region is due to the existing or evolving polar vortex. The effect of photochemistry can be considered negligible during the polar winter on latitudes poleward of 60° N. As Fig. 6 already showed, with time NO_x is transported at lower altitudes with mixing ratios of 60–80 ppb finally reaching 54 km on 15 March. ACE-FTS measurement locations are marked in the figure with filled white circles. As mentioned already in section 2.2 ACE-FTS makes about 10 measurements per day. In cases when some of the data are corrupted and excluded from the analysis, even fewer observations are left to represent the whole polar cap region. This might lead to differences between observations and the model results, especially close to the polar vortex edge. In addition, the closest model grid to ACE-FTS measurement covers by definition a larger area (10° × 5°) than the point-form observation does and can also be inside the vortex, although the measurement was made outside the vortex. This can partly explain the differences between the model and observations.

To estimate the effect of chemistry on descending NO_x, we have analysed the NO_x tracer in the model. The tracer uses the same boundary condition as NO_x, but is not affected by chemistry. Transport is thus the only factor that affects the tracer. The relative effect of chemistry can be calculated by dividing the difference between NO_x and the tracer with the
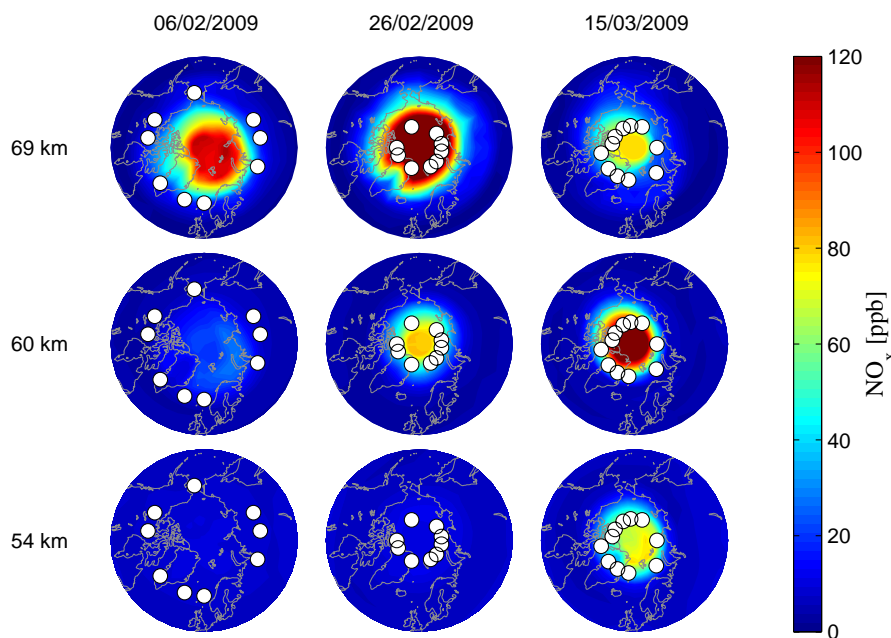
Fig. 7. Distribution of NO_x in ppb at 69, 60 and 51 km altitudes (rows) on 6 and 26 February and 15 March (columns) in the northern polar region (50° N–90° N) calculated from the model results. White circles indicate the measurement locations of ACE-FTS on that particular day.

amount of NO_x. The model results indicate that the chemical production of NO_x is not effective during polar winter and, furthermore, the relative chemical loss is only 3 % or less (not shown), meaning that chemistry does not affect the NO_x concentrations during the polar night. Therefore NO_x can descend inside the arctic vortex with only little interference by chemistry. In addition to gas phase chemistry, also photodissociation processes affect the amount of NO_x in the middle and upper atmosphere. The time period from January to March in the northern polar area is very dark leading to only weak photodissociation processes and thus to longer photochemical lifetimes. The photochemical lifetime of NO_x was nearly two months in early January decreasing to about 5 days towards the end of March in the altitude range of 60–80 km. This is a further evidence that NO_x was mainly influenced by atmospheric dynamics during the time period under investigation.

### 3.3 Effects on O_3

The descent event of NO_x in 2009 was one of the strongest observed. If transported down to the stratosphere, NO_x affects ozone balance through well-known catalytic reaction cycles (Grenfell et al., 2006). Although we do not expect to see any NO_x related changes in stratospheric ozone in this case (the descending NO_x did not reach stratosphere before vortex breakdown) we are interested in any effects this meteorological event might have had on ozone. Figure 8 shows

ACE-FTS observations and FinROSE model results of ozone in early 2009. Analysing the O_x tracer in the model (not shown), similarly to the NO_x tracer earlier, we find that the behaviour of ozone until mid-February, including ozone decrease in late January and early February, was largely determined by the dynamics. The model results show lower ozone mixing ratios around 40 km compared to the observations, which can partially be explained by the non-perfect correspondence of the closest model grid point with the daily median of the observations.

Both ACE-FTS and FinROSE show ozone decrease after mid-February 2009 starting from around 50 km (Fig. 8). The observations indicate a decrease of about 20 % between 30–50 km lasting one month and recovery in early March. In the model, ozone depletion is about 10 % stronger than observed while the recovery takes place later in mid-March. Although coinciding with the NO_x descent, the ozone decrease is not directly linked to the descent as discussed earlier. The dynamics could, on the other hand, lead to ozone decrease at 40 km through transport of low ozone concentrations from above. The O_x tracer analysis, however, indicates that transport of air with low O_x concentrations cannot explain its decrease. Similar to NO_x descent, the descent of low O_x air did not affect altitudes below 50 km. Below 50 km the downward transport was too weak to explain the observed structure of ozone. In the model, ozone destroying substances, such as HO_x, bromine and chlorine, were produced after mid-February as the solar radiation increased and
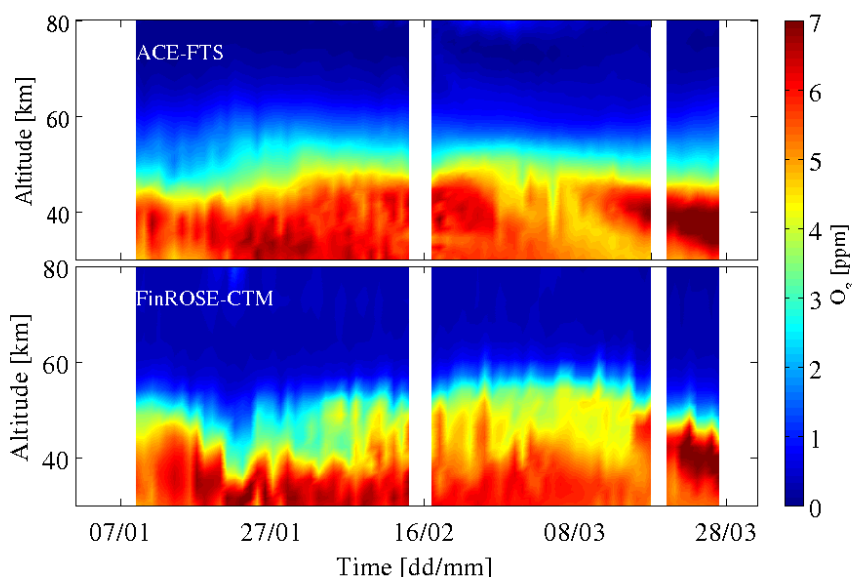
Fig. 8. ACE-FTS (top) and FinROSE-CTM (bottom) ozone time series in ppm as a function of altitude for early 2009 in ACE-FTS measurement locations.

the chemical processes, including photodissociation, started to play an important role on atmospheric composition. These substances, with the help of a strong polar vortex, enabled the catalytic cycles destroying ozone and caused the observed depletion at 40 km. When the solar radiation increased, the production of ozone began to dominate. This led to increase of ozone in both the observations and model results in early March at 45 km altitude and then gradually also at lower altitudes as shown in Fig. 8.

4 Discussion

In the case of 2009, even though a strong descent event occurred, enhanced mesospheric NO_x did not reach the upper stratosphere and thus did not affect ozone. The model results show this behaviour throughout the northern polar cap region, in agreement with the spatially limited ACE-FTS observations. However, based on a single case of descent presented in this paper, we cannot in general dismiss the possible connection between descending NO_x, upper stratospheric ozone decrease, and subsequent changes in dynamics. If the SSW had occurred earlier, NO_x would have had more time to descend and reach the stratosphere before the vortex break-up/split. According to the model results, NO_x rapidly descended from mesosphere to stratosphere with a velocity of about 700 m day^{-1} in February and early March 2009. In contrast, average descent rates in the polar vortex are typically less than 200 m day^{-1}. Assuming velocity of 700 m day^{-1}, the descent should have started 10–30 days earlier in order to reach 50–35 km altitude.

We would like to point out that Randall et al. (2009) and Vogel et al. (2008) have shown that the observed ozone loss in early 2004 can be attributed to a NO_x descent event similar to that of 2009. Compared to the 2009 event, the SSW that caused the NO_x descent in early 2004 occurred about one month earlier, i.e. in late December, allowing enhanced NO_x to reach the stratosphere. Therefore, strong NO_x descent events seem to decrease stratospheric ozone only if the corresponding SSW occurs early enough in the winter period (by ∼early January), although this time condition would obviously be relaxed if in-situ production of NO_x by energetic particle precipitation occurred at altitudes below 80 km. If the SSW occurred later than early January, it might actually lead to weaker connection between MLT NO_x production and stratospheric ozone, i.e. any enhanced NO_x amounts already in the mesosphere would be mixed with outside-vortex air during the SSW, and the after-SSW descent would start too late to transport NO_x from the upper mesosphere to the stratosphere, as in the case of the 2009 descent event. In such conditions, the effect of EEP-NO_x on stratospheric ozone in SSW years could be equal or smaller compared to years without a SSW. This could be one potential reason for the findings of Lu et al. (2008) and Seppälä et al. (2009), who have demonstrated that changes in stratospheric and tropospheric dynamics actually correlate with geomagnetic Ap index better when the SSW-years were excluded from their analyses. It is evident to us that more research is needed to answer the questions concerning NO_x–O_3 interaction and possible connection to stratospheric/tropospheric dynamics.

5 Conclusions

In this paper, we have used the FinROSE-CTM and ACE-FTS observations to study the effect of polar vortex dynamics on the distribution of NO_x in the winter polar region. Two different Northern Hemisphere cases, 2007 and 2009, were considered. The latter was characterized by a strong NO_x descent event in February–March, which begun after a record-breaking SSW. In the modelling, we used ECMWF operational winds, temperature, and pressure up to 0.01 hPa ($\sim$80 km) and a NO_x upper boundary at 80 km based on ACE-FTS observations, and then compared the results with the observations at lower altitudes.

In contrast to 2007, when a SSW did not have any significant effects on the atmospheric composition, in 2009 large amounts of NO_x descended from the upper mesosphere to the stratosphere following a major SSW. Analysis of ECMWF data shows that the descent was enabled by the formation of a strong polar vortex facilitated by easterly zonal flow that prevented the vertical propagation of planetary waves. Based on ACE-FTS observations, the NO_x descent continued until mid-March, by which time the high-NO_x amounts of 150–200 ppb reached down to 55 km. The FinROSE-CTM results are in reasonable agreement with ACE-FTS, except that the amount of NO_x at 55 km is underestimated by 40–60 ppb compared to the observations. Although the ACE-FTS observations have a restricted spatial coverage, the model results indicate that the measurements give a good representation of the NO_x descent throughout the polar cap. The FinROSE-CTM results also show that chemical production and loss of NO_x was insignificant during the descent in the polar night region, so that NO_x distribution was controlled by the vortex dynamics. The reasonably good agreement between observations and the model gives confidence in the usability of the ECMWF operational data in mesospheric modelling.

Although a strong descent event occurred in February–March 2009 after a major SSW, we find that in this case the high NO_x amounts did not reach upper stratosphere and thus did not catalytically deplete ozone. Instead, both ACE-FTS and FinROSE-CTM show ozone decreased by about 20 % at 30–50 km in late February–early March, which according to the model was due to increasing amount of solar radiation and activation of HO_x and halogen compounds. However, if a similar descent event had begun about a month earlier, NO_x would have reached stratospheric altitudes. Therefore, it seems that a connection between EEP-NO_x production in the MLT region and stratospheric ozone variability requires suitable timing of descent events, and our case study does not exclude the possibility of this connection. More research on EPP-NO_x and stratospheric ozone is needed, keeping in mind the links to dynamics and ground-level temperature and pressure anomalies that have been suggested.

References

Arnold, N. F. and Robinson, T. R.: Solar magnetic flux influences on the dynamics of the winter middle atmosphere, Geophys. Res. Lett., 28(12), 2381–2384, doi:10.1029/2000GL012825, 2001.

Barth, C. A.: Nitric oxide in the lower thermosphere, Planet. Space Sci., 40, 315–336, 1992.

Baumgaertner, A. J. G., Jöckel, P., and Brühl, C.: Energetic particle precipitation in ECHAM5/MESSy1 – Part 1: Downward transport of upper atmospheric NOx produced by low energy electrons, Atmos. Chem. Phys., 9, 2729–2740, doi:10.5194/acp-9-2729-2009, 2009.

Baumgaertner, A. J. G., Seppälä, A., Jöckel, P., and Clilverd, M. A.: Geomagnetic activity related NOx enhancements and polar surface air temperature variability in a chemistry climate model: modulation of the NAM index, Atmos. Chem. Phys. Discuss., 10, 30171–30203, doi:10.5194/acpd-10-30171-2010, 2010.

Bernath, P. F., McElroy, C. T., Abrams, M. C., Boone, C. D., Butler, M., Camy-Peyret, C., Carleer, M., Clerbaux, C., Coheur, P.-F., Colin, R., DeCola, P., DeMaziére, M., Drummond, J. R., Dufour, D., Evans, W. F. J., Fast, H., Fussen, D., Gilbert, K., Jennings, D. E., Llewellyn, E. J., Lowe, R. P., Mahieu, E., McConnell, J. C., McHugh, M., McLeod, S. D., Michaud, R., Midwinter, C., Nassar, R., Nichitiu, F., Nowlan, C., Rinsland, C. P., Rochon, Y. J., Rowlands, N., Semeniuk, K., Simon, P., Skelton, R., Sloan, J. J., Soucy, M.-A., Strong, K., Tremblay, P., Turnbull, D., Walker, K. A., Walkty, I., Wardle, D. A., Wehrle, V., Zander, R., and Zou, J.: Atmospheric Chemistry Experiment (ACE): Mission overview, Geophys. Res. Lett., 32, L15S01, doi:10.1029/2005GL022386, 2005.

Callis, L. B. and Lambeth, J. D.: NOy formed by precipitating electron events in 1991 and 1992: Descent into the stratosphere as observed by ISAMS, Geophys. Res. Lett., 25, 1875–1878, doi:10.1029/98GL01219, 1998.

Callis, L. B., Natarajan, M., and Lambeth, J. D.: Calculated upper stratospheric effects of solar UV flux and NOy variations during the 11-year solar cycle, Geophys. Res. Lett., 27(23), 3869–3872, doi:10.1029/2000GL011622, 2000.

Callis, L. B., Natarajan, M., and Lambeth, J. D.: Solar-atmospheric coupling by electrons (SOLACE) 3, Comparisons of simulations and observations, 1979-1997, issues and implications, J. Geophys. Res., 106, 7523–7539, doi:10.1029/2000JD900615, 2001.

Clilverd, M. A., Seppälä, A., Rodger, C. J., Verronen, P. T., and Thomson, N. R.: Ionospheric evidence of thermosphere-

to-stratosphere descent of polar NO$_x$, Geophys. Res. Lett., 33, L19811, doi:10.1029/2006GL026727, 2006.

Damski, J., Thölix, L., Backman, L., Taalas, P. and Kulmala, M.: FinROSE – middle atmospheric chemistry transport model, Boreal Env. Res., 12, 535–550, 2007.

Funke, B., Lopéz-Puertas, M., Gil-López, S., von Clarmann, T., Stiller, G. P., Fischer, H., and Kellmann, S.: Downward transport of upper atmospheric NO$_x$ into the polar stratosphere and lower mesosphere during the Antarctic 2003 and Arctic 2002/2003 winters, J. Geophys. Res., 110, D24308, doi:10.1029/2005JD006463, 2005.

Funke, B., Lopéz-Puertas, M., Fischer, H., Stiller, G. P., von Clarmann, T., Wetzel, G., Carli, B., and Belotti, C.: Comment on "Origin of the January–April 2004 increase in stratospheric NO$_2$ observed in northern polar latitudes", by: Jean-Baptiste Renard et al., Geophys. Res. Lett., 34, L07813, doi:10.1029/2006GL027518, 2007.

Grenfell, J. L., Lehmann, R., Mieth, P., Langematz, U., and Steil, B.: Chemical reation pathways affecting stratospheric and mesospheric ozone, J. Geophys. Res., 111, D17311, doi:10.1029/2004JD005713, 2006.

Hauchecorne, A., Bertaux, J.-L., Dalaudier, F., Russell III, J. M., Mlynczak, M. G., Kyrölä, E., and Fussen, D., : Large increase of NO$_2$ in the north polar mesosphere in January–February 2004: Evidence of a dynamical origin from GOMOS/ENVISAT and SABER/TIMED data, Geophys. Res. Lett., 34, L03810, doi:10.1029/2006GL027628, 2007.

Kylling, A., Albold, A. and Seckmeyer, G.: Transmittance of a cloud is wavelength – dependent in the UV-range: Physical interpretation, Geophys. Res. Lett., 24(4), 397–400, doi:10.1029/97GL00111, 1997.

Langematz, U., Grenfell, J. L., Matthes, K., Mieth, P., Kunze, M., Steil, B., and Brühl, C.: Chemical effects in 11-year solar cycle simulations with the Freie Universität Berlin Climate Middle Atmosphere Model with online chemistry (FUB-CMAM-CHEM), Geophys. Res. Lett., 32, L13803, doi:10.1029/2005GL022686, 2005.

Lu, H., Clilverd, M. A., Seppälä, A., and Hood, L. L.: Geomagnetic perturbations on stratospheric circulation in late winter and spring, J. Geophys. Res., 113, D16106, doi:10.1029/2007JD008915, 2008.

Manney, G. L., Daffer, W. H., Strawbridge, K. B., Walker, K. A., Boone, C. D., Bernath, P. F., Kerzenmacher, T., Schwartz, M. J., Strong, K., Sica, R. J., Krüger, K., Pumphrey, H. C., Lambert, A., Santee, M. L., Livesey, N. J., Remsberg, E. E., Mlynczak, M. G., and Russell III, J. R.: The high Arctic in extreme winters: vortex, temperature, and MLS and ACE-FTS trace gas evolution, Atmos. Chem. Phys., 8, 505–522, doi:10.5194/acp-8-505-2008, 2008.

Manney, G. L., Schwartz, M. J., Krüger, K., Santee, M. L., Pawson, S., Lee, J. N., Daffer, W. H., Fuller, R. A., and Livesey, N. J.: Aura Microwave Limb Sounder observations of dynamics and transport during the record-breaking 2009 Arctic stratosphere major warming, Geophys. Res. Lett., 36, L12815, doi:10.1029/2009GL038586, 2009.

McInturff, R.: Stratospheric warmings: Synoptic, dynamic and general-circulation aspects, NASA Reference Publ. NASA-RP-1017, NASA, Natl. Meteorol. Cent., Washington, DC, 1978.

Randall, C. E., Harvey, V. L., Siskind, D. E., France, J., Bernath, P. F., Boone, C. D., and Walker, K. A.: NO$_x$ descent in the Arctic middle atmosphere in early 2009, Geophys. Res. Lett., 36, L18811, doi:10.1029/2009GL039706, 2009.

Reddmann, T., Ruhnke, R., Versick, S., and Kouker, W.: Modeling disturbed stratospheric chemistry during solar-induced NO$_x$ enhancements observed with MIPAS/ENVISAT, J. Geophys. Res., 115, D00I11, doi:10.1029/2009JD012569, 2010.

Rozanov, E., Callis, L., Schlesinger, M., Yang, F., Andronova, N., and Zubov, V.: Atmospheric response to NO$_y$ source due to energetic electron precipitation, Geophys. Res. Lett., 32, L14811, doi:10.1029/2005GL023041, 2005.

Sander, S. P., Friedl, R. R., Golden, D. M., Kurylo, M. J., Moortgat, G. K., Keller-Rudek, H., Wine, P. H., Ravishankara, A. R., Kolb, C. E., Molina, M. J., Finlayson-Pitts, B. J., Huie, R. E., and Orkin, V. L.: Chemical kinetics and photochemical data for Use in Atmospheric Studies, Evaluation Number 15, Publication 06-2, JPL, Pasadena, USA, 2006.

Seppälä, A., Verronen, P. T., Clilverd, M. A., Randall, C. E., Tamminen, J., Sofieva, V., Backman, L., and Kyrölä, E.: Arctic and Antarctic polar winter NO$_x$ and energetic particle precipitation in 2002–2006, Geophys. Res. Lett., 34, L12810, doi:10.1029/2007GL029733, 2007.

Seppälä, A., Randall, C., Clilverd, M. A., Rozanov, E., and Rodger, C. J.: Geomagnetic activity and polar surface air temperature variability, J. Geophys. Res., 114, A10312, doi:10.1029/2008JA014029, 2009.

Siskind, D. E., Bacmeister, J. T., Summers, M. E., and Russell III, J. M.: Two-dimensional model calculations of nitric oxide transport in the middle atmosphere and comparison with Halogen Occultation Experiment data, J. Geophys. Res., 102, 3527–3546, doi:10.1029/96JD02970, 1997.

Solomon, S., Crutzen, P. J., and Roble, R. G.: Photochemical coupling between the thermosphere and the lower atmosphere: 1. odd nitrogen from 50 to 120 km, J. Geophys. Res., 87(C9), 7206–7220, 1982.

Vitt, F. M., Armstrong, T. P., Cravens, T. E., Dreschhoff, A. M., Jackman, C. H., and Laird, C. M.: Computed contributions to odd nitrogen concentrations in the Earth's polar middle atmosphere by energetic charged particles, J. Atmos. Sol.-Terr. Phys., 62, 669–683, 2000.

Vogel, B., Konopka, P., Grooß, J.-U., Müller, R., Funke, B., López-Puertas, M., Reddmann, T., Stiller, G., von Clarmann, T., and Riese, M.: Model simulations of stratospheric ozone loss caused by enhanced mesospheric NO$_x$ during Arctic Winter 2003/2004, Atmos. Chem. Phys., 8, 5279–5293, doi:10.5194/acp-8-5279-2008, 2008.